ACS Photonics

Letter

pubs.acs.org/journal/apchd5

Topological Majorana States in Zigzag Chains of Plasmonic Nanoparticles

Alexander Poddubny,[†,‡] Andrey Miroshnichenko,[*,§] Alexey Slobozhanyuk,[‡] and Yuri Kivshar[‡,∥]

[†]Ioffe Physical-Technical Institute of the Russian Academy of Sciences, St. Petersburg 194021, Russia

[‡]National Research University for Information Technology, Mechanics and Optics (ITMO), St. Petersburg 197101, Russia

[§]Nonlinear Physics Centre, Research School of Physics and Engineering and [∥]Nonlinear Physics Centre and Centre for Ultrahigh-Bandwidth Devices for Optical Systems (CUDOS), Research School of Physics and Engineering, Australian National University, Canberra ACT 0200, Australia

ABSTRACT: We propose a simple realization of topological edge states in zigzag chains of plasmonic nanoparticles, mimicking the Kitaev model of Majorana fermions. We demonstrate the one-to-one correspondence between the coupled dipole equations in the zigzag plasmonic chain and the Bogoliubov-de-Gennes equations for the quantum wire on top of superconductor and support the analytical theory by the full-wave electromagnetic simulations. We reveal that localized plasmons can be excited selectively at both edges of the zigzag chain of plasmonic nanoparticles depending on the incident plane wave polarization.

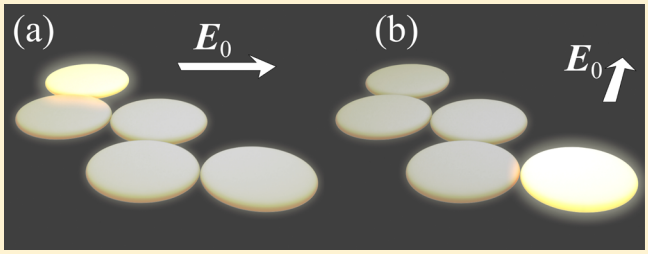

KEYWORDS: *topological insulators, edge states, plasmonics, Majorana fermions*

The study of topological insulators is one of the most rapidly developing areas of condensed matter physics.[1,2] Such structures possess bandgaps in the bulk and special edge/surface states inside the gap. Contrary to traditional Tamm states, these edge states are topologically protected. This means that they are stable against a wide class of perturbations that keep a general symmetry of the system,[3] for example, time-reversal symmetry or particle-hole symmetry. Recently, a significant progress has been made in the study of the topological edge states of photons in various structures, such as photonic crystals,[4,5] coupled cavities,[6] waveguide arrays,[7−9] photonic quasicrystals,[10,11] and metamaterials.[12] Robust optical topological edge states are promising candidates for future optical transmission lines, surviving under any disorder.[6]

In this Letter, we introduce and analyze the topological states in the chains of plasmonic nanoparticles. Plasmonic clusters of different shapes demonstrate rich physics,[13−18] and their point symmetry can be probed by analyzing the scattering spectra.[19] Our goal is to draw attention to the topological symmetry of the clusters. We demonstrate a one-to-one correspondence between the coupled localized plasmon modes in zigzag clusters and the Majorana edge states of the Kitaev's model for the quantum wire on top of superconductor.[20] Majorana fermions are unique fermionic particles being their own antiparticles,[21] they are now actively sought in solids[22] as well as in optics,[23] and they are potential candidates to realize robust qubits.[20] Here we uncover additional symmetries of the zigzag chains, stemming from the vector nature of the dipole−dipole interaction, and show that plasmonic structures are promising candidates to mimic fascinating Majorana physics.

The structure under consideration is schematically shown in Figure 1. It presents a finite zigzag chain of $j = 1, ..., N$ plasmonic disks lying in the xy plane.

$$\mathbf{r}_j = \begin{cases} L\dfrac{j-1}{2}(\hat{\mathbf{x}} + \hat{\mathbf{y}}), & (\text{odd } j) \\ L\dfrac{j}{2}(\hat{\mathbf{x}} + \hat{\mathbf{y}}) - L\hat{\mathbf{y}}, & (\text{even } j) \end{cases} \tag{1}$$

The chain has the period $L(\hat{\mathbf{x}} + \hat{\mathbf{y}})$ and each unit cell contains two nanodisks of the radius R and the height h.

The simplest technique to determine the optical response is to employ eigenmode decomposition. The system eigenmodes for subwavelength nanoparticles is can be found based on the electric dipole approximation:[24,25]

$$\mathbf{p}_j = \hat{\alpha} \sum_{j'} \hat{G}(\mathbf{r}_j - \mathbf{r}_{j'})\mathbf{p}_{j'} \tag{2}$$

Here, $\mathbf{p}_j$ is the dipole moment of jth particle, $\hat{\alpha}$ is the polarizability tensor with nonzero components $\alpha_{xx} = \alpha_{yy} = \alpha_{\parallel}$, $\alpha_{zz} = \alpha_{\perp}$, and $\hat{G}(r)$ is the tensor Green function. Equation 2 can be solved numerically for an arbitrary geometry. However, it turns out that for the particular zigzag arrangement eq 1, with the angle between the nearest "bonds" is equal to 90°, the coupled plasmonic eigenstates have special symmetry properties. To demonstrate this effect, we include only nearest-neighbor interactions in the dipole−dipole approximation with

Received: October 27, 2013
Published: January 14, 2014

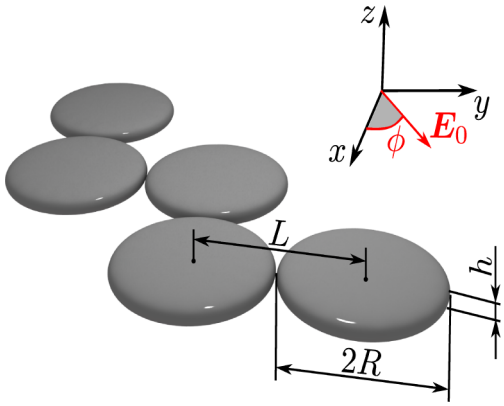

Figure 1. Schematics of a zigzag array of plasmonic nanoparticles.

$$\hat{G}(\mathbf{r}) = \frac{3\mathbf{r} \otimes \mathbf{r} - r^2}{r^5} \tag{3}$$

We also focus on the normal wave incidence, when the field propagates along z direction. In this case, all the excited dipole momenta lie in the xy plane and can be described in the following basis

$$\mathbf{p}_j = u_j \mathbf{e}_u(j) + v_j \mathbf{e}_v(j) \tag{4}$$

$$\mathbf{e}_u(j) = -\cos\phi_j \hat{\mathbf{x}} + \sin\phi_j \hat{\mathbf{y}},\ \mathbf{e}_v(j) = -\sin\phi_j \hat{\mathbf{x}} - \cos\phi_j \hat{\mathbf{y}}$$

$$\phi_j = \pi j/2$$

We also use the pole approximation for the particle polarizability $\alpha_{\parallel} = \Gamma_{\parallel}/(\omega_0 - \omega)$, valid near the plasmon resonance frequency ω_0. Substituting 4 and 3 into 2, we obtain the homogeneous system of equations for coupled plasmonic eigenmodes

$$(\omega - \omega_0)u_j = t(u_{j+1} + u_{j-1}) + \Delta(v_{j+1} - v_{j-1}) \tag{5}$$

$$(\omega - \omega_0)v_j = -t(v_{j+1} + v_{j-1}) - \Delta(u_{j+1} - u_{j-1})$$

where

$$t = \frac{3\Gamma_{\parallel}}{2L^3},\ \Delta = -\frac{\Gamma_{\parallel}}{2L^3} \tag{6}$$

Equations 5 have a striking similarity to the Bogoliubov-de-Gennes equations of Kitaev's model, describing the quasi-particles in the quantum wire lying on top of the superconductor.[20] In the original Kitaev's Hamiltonian $H = (1/2)\sum_j (tc_j^{\dagger}c_{j+1} + \Delta c_j c_{j+1}) + h.c$, the constant t is the transfer integral describing the motion along the wire, while Δ is the superconducting gap, and c_j ($c_j^{\dagger}$) are the electron annihilation (creation) operators for the site j. In our case, the role of particle-hole excitations is taken by the two polarization degrees of freedom. Similar models also appear for coupled waveguides,[26,27] chains of defects inside the photonic crystals,[28] and conjugated polymer chains.[29] The general properties of the system eq 5 can be understood in the special particular case when $\Delta = -t$. For such parameters, the spectrum contains only three eigenfrequencies, $\omega_0 \pm 2t$ and ω_0. All the $2N$ corresponding eigenmodes for the zigzag with N disks are schematically illustrated in Figure 2. The mode shown in Figure 2a, Figure 2d has the frequency

$$\omega_{\text{bright}} = \omega_0 - 2t \tag{7}$$

and the total degeneracy $N - 1$. Because the dipole momenta on the neighboring disks are parallel to each other, this mode is bright, that is, it can be excited by a normally incident plane wave. Conversely, the mode in Figure 2c,e is dark, has the frequency $\omega_{\text{dark}} = \omega_0 + 2t$, and the same total degeneracy $N - 1$. The remaining eigenmode is shown in Figure 2b. It has the frequency

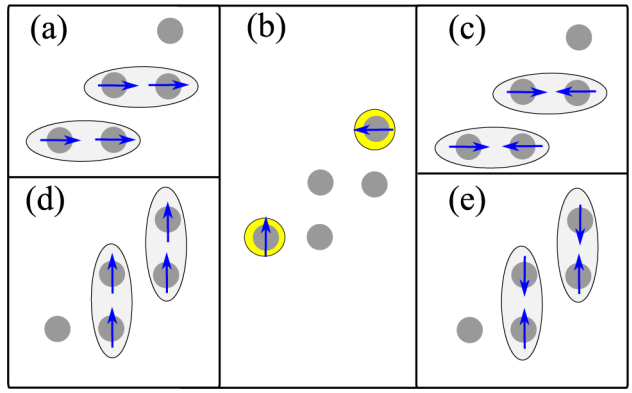

Figure 2. Illustration of the dipole eigenmodes of eq 5 for $\Delta = -t$.

$$\omega_{\text{loc}} = \omega_0 \tag{8}$$

corresponding to the single-particle resonance. This is an edge eigenmode with nonzero momenta only at the first and last disks. The mode is doubly degenerate, the y-polarized dipole momentum corresponds to the first disk, x-polarized to the last one. Indeed, while for $j = 2, ..., N - 1$ the in-plane dipole momentum is coupled to one of the modes at Figure 2a or c, the y- and x-polarized modes of the first and last particles remain uncoupled and, hence, are localized.

It has been shown[20] that the structure of the eigenmodes remains qualitatively the same for arbitrary values of $\Delta \neq 0$. Particularly, the degenerate bright and dark modes at $\omega = \omega_0 \pm 2t$ evolve into the two allowed bands with the dispersion $\omega(K) = \omega_0 \pm 2(t^2 \cos^2 K + \Delta^2 \sin^2 K)^{1/2}$. Here, K is the Bloch wavevector, $u_{j+1} = e^{iK}u_j$. The frequency of the double-degenerate state 8 is equal to ω_0 independent of Δ. For $|\Delta| \neq 0$ this state is exponentially localized at the structure edges, the case when $\Delta = -t/3$ corresponds to the edge states decaying as $|p_j|^2 \propto 1/2^{|j|}$.

Appearance of the edge states may be understood as the topological transition taking place when the chain geometry changes from a line to a zigzag. Such zigzag distortion is a particular kind of the Peierls phase transition.[31]

The simple analysis above suggests the presence of localized polarization-degenerate plasmonic eigenmodes in the zigzag chain at the frequency corresponding to the resonance of the single disk. To confirm this hypothesis we numerically simulate the electric field induced in the structure by the plane wave $\underline{E}_0 e^{ikz}$, propagating along z direction at different frequencies. The calculation has been performed using the CST Microwave Studio software for touching nanodisks $L = 2R$. Electric field is linearly polarized, $\boldsymbol{E}_0 = \cos\phi\hat{\mathbf{x}} + \sin\phi\hat{\mathbf{y}}$ with $\phi = 45°$. The results of calculation are demonstrated in Figure 3. Thick/black curve in the panel (a) shows numerically calculated extinction cross section for the zigzag chain with 11 nanodisks. Thin/red curve presents the cross section for a single disk, which has the dipole resonance at the energy $E \approx 2.1$ eV. The cross section for the zigzag chain has a complex multipeak structure. Main peak in the spectrum is blue-shifted from the single disk resonance, in

dx.doi.org/10.1021/ph4000949 | ACS Photonics 2014, 1, 101−105

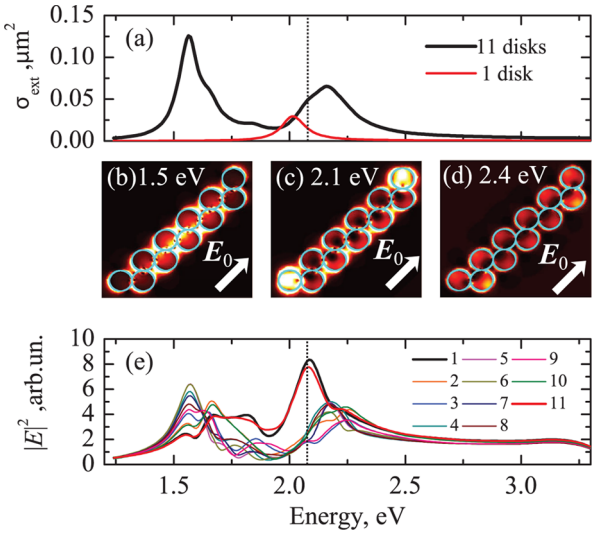

Figure 3. (a) Extinction cross section spectrum for a zigzag chain with 11 silver nanodisks (thick/black curve) and for single disk (thin/red curve). (b–d) False color maps of the electric field intensity at the different energies, indicated in the panels. (e) Energy dependence of the squared electric field in the centers of the disks. Vertical dotted line in panels (a) and (e) denotes the energy $E \approx 2.1$ eV, where the field localization at the zigzag edges takes place. Calculation was performed for touching nanodisks with $R = 30$ nm, $h = 3$ nm, $\phi = 45°$. Dielectric constant of silver was taken from ref 30.

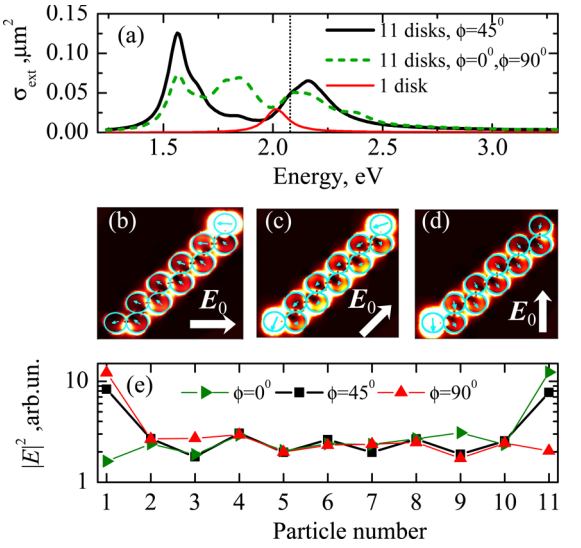

Figure 4. (a) Extinction cross section spectrum for the zigzag with 11 disks calculated at $\phi = 45°$ (solid/black curve) and at $\phi = 0°$, 90° (dashed/green curve). Thin/red curve corresponds to the extinction for a single disk. (b–d) False color maps of the electric field intensity at $E = 2.1$ eV and different incident wave polarizations $\phi = 0°$, 45°, and 90°, respectively, indicated in the panels by white arrows. Cyan arrows schematically illustrate the real parts of the dipole momenta induced in the particles. (e) Dependence of the electric field in the particle center on the particle number for $\phi = 0°$ (green triangles), 45° (squares), and 90° (red triangles) at $E = 2.1$ eV. Lines are guide for eye. Other parameters are the same as in Figure 3

agreement with eq 7 for the bright mode eigenfrequency. The results of the analysis of the electric field distribution, excited inside the cluster at the different frequencies, are presented in the panels (b–e). Panels (b)–(d) show the false color maps of the electric field in the xy plane, while panel (e) shows the frequency dependence of the electric field at the center of each particle. At low (b) or large (d) frequencies, the induced electric field is relatively homogeneously distributed inside the cluster. However, at the central frequency (panel c) the field has strong maxima at the first and last particles. This is also demonstrated by Figure 3e. Black and dark blue curves, corresponding to $j = 1$ and $j = 11$ have maxima at the single particle resonance $E \approx 2.1$ eV, which is a direct manifestation of the excitation of localized states.

Next, we examine the polarization dependence of the structure response. Figure 4 presents the spatial distribution of the polarization, excited at $E = 2.1$ eV for three different values of the angle $\phi = 0$, 45°, and 90° between the electric field direction and the x axis. Panel (a) shows the polarization dependence of the extinction cross section. The black line presents the extinction cross section for $\phi = 45°$, green curve shows the result for $\phi = 0$. Since the structure has mirror plane $x = -y$, the cross section for $\phi = 0$ and 90° is the same. Panels (b–e) illustrate the polarization dependence of the induced electric field pattern.

Clearly, the direction of the incident wave polarization controls the distribution of the field at the structure edges. Particularly, for the x polarization ($\phi = 0$) the field is localized at the last particle, $j = 11$, while for the y polarization ($\phi = 90°$) the field is localized at the first particle, in agreement with Figure 2b. The effect is clearly manifested both in the color maps of the field (panels b and d) and in the spatial distribution of the field in the particle centers (green and red curves in panel e). The dipole momenta of the particles, extracted from the electric field distribution, are directed oppositely to the electric field (cyan arrows in panels b–d). The case when $\phi = 45°$ corresponds to equal amplitudes for both particles (panel c and black line in panel e). Hence, the presence of the polarization-degenerate eigenmode at $E \approx 2.1$ eV allows selective excitation of the first or the last disk. This is an optical analogue of a qubit, based on Majorana fermions, proposed by Kitaev.[20] Here, the polarization switching has a purely classical origin. The truly quantum regime, where the bosonic properties of the edge states become manifested, may demonstrate even richer physics. For instance, similar systems with tunneling-coupled cavities are already used for polarization-entangled photon pair generation[32] and are proposed for quantum computing devices with multipartite entanglement.[33]

It is also instructive to examine the degree of the states localization as function of the number of particles in the chain. The results for $N = 3, ..., 6, 10$, and 11 are shown in Figure 5. This

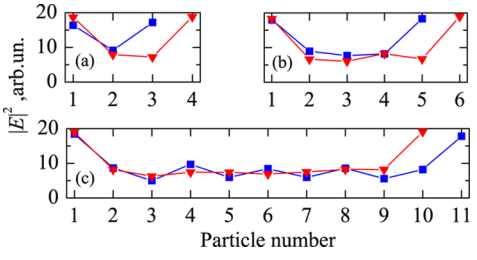

Figure 5. Dependence of the electric field in the particle center on the particle number for zigzags with $N = 3, 4$ (a), $N = 5, 6$ (b), $N = 10, 11$ (c) disks. Lines are guide for eye. Calculation was performed at $E \approx 2.1$ eV, $\phi = 45°$, and the same other parameters as in Figure 3

figure demonstrates that the edge states are manifested already for the smallest possible structure with defined edges, that is, for the zigzag chain with $N = 3$ particles. Importantly, the localization takes place at the same frequency independent of the structure

dx.doi.org/10.1021/ph4000949 | ACS Photonics 2014, 1, 101–105

length. Localization has a compact character: its strength slowly increases when the number of particles grows but saturates already at $N \approx 5$. The maximum edge-to-center ratio of the field intensities, $|E_1|^2/|E_6|^2$ is about three. Thus, the localization is weaker than exponential, contrary to the traditional Kitaev model. The reason is that the direct correspondence between the Kitaev model and the considered model is valid only for the nearest-neighbor dipole−dipole interactions. The long-ranged electromagnetic coupling between the nanodisks partially suppresses the localization.

Figure 6 examines the robustness of the edge states against the disorder. Panels (a) and (b) are calculated for the ideal structure,

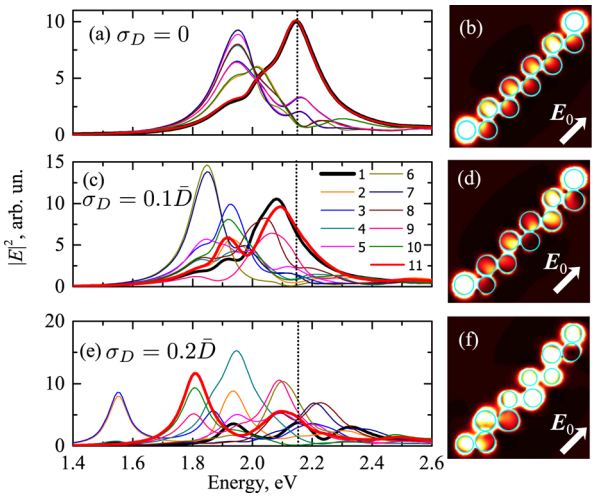

Figure 6. Effect of disorder on the edge states. (a, b) Ideal structure; (c−f) disordered structures with dispersion of disk diameter and position (c, d) $\sigma_D = 0.1\bar{D} = 5$ nm and (e, f) $\sigma_D = 0.2\bar{D} = 10$ nm. (a, c, e) Energy dependence of the squared electric field in the disk centers. Vertical dotted line denotes the energy $E \approx 2.15$ eV, corresponding to the single disk resonance. (b−d) False color maps of the electric field intensity. Calculated for $\phi = 45°$, $\bar{D} = 50$ nm, $\bar{L} = 60$ nm, and the same other parameters as in Figure 3.

where all the disk diameters are equal to $\bar{D} = 50$ nm and the center-to-center distance is $\bar{L} = 60$ nm. Results are qualitatively the same as in Figure 3: at the single disk resonance energy $E \approx 2.15$ eV mainly the first and last particles are excited. We include the disorder both in the positions and in the diameter of the disks. This leads to the inhomogeneous broadening of the dipole resonances and to the modification of the coupling between the disks due to the random distortion of the zigzag chain. Particularly, we assume that the in-plane disk center coordinates x and y and the disk diameter are independent random Gaussian variables, characterized with the same dispersion σ_D. Figure 6c−f is calculated for two realizations of the disorder with different strengths, $\sigma_D = 0.1\bar{D} = 5$ nm and $\sigma_D = 0.2\bar{D} = 10$ nm. The impact of the disorder on the excited electric field distribution is significant already for $\sigma_D = 0.1\bar{D}$, see Figure 6a,c. However, the edge states still survive in this case. This is illustrated by Figure 6d, which demonstrates preferential excitation of the edges of the disordered chain at the frequency of the single disk resonance of the ideal structure. Edge states are completely destroyed only for strong disorder, $\sigma_D = 0.2\bar{D}$, when the chain mode structure is changed completely, see Figure 6e,f.

In summary, we have proposed a simple plasmonic analogue of the concept of Majorana topological edge states in the zigzag chain of metallic nanodisks. We have demonstrated an exact correspondence between Kitaev's model of a finite-extent quantum wire over superconductor to the model of coupled electric dipoles in the plasmonic chain. This mapping is valid for the dipole−dipole interactions between the nearest neighbors of the chain. The edge states have been shown to be robust against distant interactions and disorder. We have demonstrated the possibility to excite selectively two edges of the zigzag chain by changing the direction of the linear polarization of the incident light. We believe that the study of the topological properties of the polarization-entangled eigenmodes suggests a new way for engineering the properties of plasmonic clusters for novel applications in nanophotonics.

AUTHOR INFORMATION

Corresponding Author

*E-mail: andrey.miroshnichenko@anu.edu.au.

Notes

The authors declare no competing financial interest.

ACKNOWLEDGMENTS

This work was supported by the Ministry of Education and Science of Russian Federation under Grant Nos. 11.G34.31.0020, 11.519.11.2037, 14.B37.21.0307, 01201259765, by Government of Russian Federation (Grant 074-U01), the "Dynasty" Foundation, Russian Foundation for Basic Research, EC Projects POLAPHEN and SPANLG4Q, and the Australian Research Council via Future Fellowship program (FT110100037). The authors acknowledge useful discussions with E. L. Ivchenko, A. V. Poshakinskiy, A. A. Sukhorukov, S. S. Kruk, and A. Amo.

REFERENCES

(1) Hasan, M. Z.; Kane, C. L. Colloquium: Topological insulators. *Rev. Mod. Phys.* **2010**, *82*, 3045−3067.
(2) Qi, X.-L.; Zhang, S.-C. Topological insulators and superconductors. *Rev. Mod. Phys.* **2011**, *83*, 1057−1110.
(3) Kitaev, A. Periodic table for topological insulators and superconductors. *AIP Conf. Proc.* **2009**, *1134*, 22−30.
(4) Haldane, F. D. M.; Raghu, S. Possible realization of directional optical waveguides in photonic crystals with broken time-reversal symmetry. *Phys. Rev. Lett.* **2008**, *100*, 013904.
(5) Wang, Z.; Chong, Y. D.; Joannopoulos, J. D.; Soljačić, M. Reflection-free one-way edge modes in a gyromagnetic photonic crystal. *Phys. Rev. Lett.* **2008**, *100*, 013905.
(6) Hafezi, M.; Demler, E. A.; Lukin, M. D.; Taylor, J. M. Robust optical delay lines with topological protection. *Nat. Phys.* **2011**, *7*, 907−912.
(7) Kitagawa, T.; Broome, M. A.; Fedrizzi, A.; Rudner, M. S.; Berg, E.; Kassal, I.; Aspuru-Guzik, A.; Demler, E.; White, A. G. Observation of topologically protected bound states in photonic quantum walks. *Nat. Commun.* **2012**, *3*.
(8) Rechtsman, M. C.; Plotnik, Y.; Zeuner, J. M.; Song, D.; Chen, Z.; Szameit, A.; Segev, M. Topological creation and destruction of edge states in photonic graphene. *Phys. Rev. Lett.* **2013**, *111*, 103901.
(9) Rechtsman, M. C.; Zeuner, J. M.; Plotnik, Y.; Lumer, Y.; Podolsky, D.; Dreisow, F.; Nolte, S.; Segev, M.; Szameit, A. Photonic Floquet topological insulators. *Nature* **2013**, *496*, 196−200.
(10) Kraus, Y. E.; Zilberberg, O. Topological equivalence between the Fibonacci quasicrystal and the Harper model. *Phys. Rev. Lett.* **2012**, *109*, 116404.
(11) Verbin, M.; Zilberberg, O.; Kraus, Y. E.; Lahini, Y.; Silberberg, Y. Observation of topological phase transitions in photonic quasicrystals. *Phys. Rev. Lett.* **2013**, *110*, 076403.

(12) Khanikaev, A. B.; Hossein Mousavi, S.; Tse, W.-K.; Kargarian, M.; MacDonald, A. H.; Shvets, G. Photonic topological insulators. *Nat. Mater.* **2013**, *12*, 233−239.
(13) Maier, S. A. *Plasmonics: Fundamentals and Applications*; Springer: New York, 2007.
(14) Hentschel, M.; Dregely, D.; Vogelgesang, R.; Giessen, H.; Liu, N. Plasmonic oligomers: The role of individual particles in collective behavior. *ACS Nano* **2011**, *5*, 2042−2050.
(15) Francescato, Y.; Giannini, V.; Maier, S. A. Plasmonic systems unveiled by fano resonances. *ACS Nano* **2012**, *6*, 1830−1838.
(16) Noskov, R. E.; Belov, P. A.; Kivshar, Y. S. Subwavelength modulational instability and plasmon oscillons in nanoparticle arrays. *Phys. Rev. Lett.* **2012**, *108*, 093901.
(17) Frimmer, M.; Coenen, T.; Koenderink, A. F. Signature of a Fano resonance in a plasmonic metamolecule's local density of optical states. *Phys. Rev. Lett.* **2012**, *108*, 077404.
(18) Hopkins, B.; Liu, W.; Miroshnichenko, A. E.; Kivshar, Y. S. Optically isotropic responses induced by discrete rotational symmetry of nanoparticle clusters. *Nanoscale* **2013**, *5*, 6395−6403.
(19) Bao, K.; Mirin, N. A.; Nordlander, P. Fano resonances in planar silver nanosphere clusters. *Appl. Phys. A* **2010**, *100*, 333−339.
(20) Kitaev, A. Y. Unpaired Majorana fermions in quantum wires. *Phys.-Usp.* **2001**, *44*, 131.
(21) Wilczek, F. Majorana returns. *Nat. Phys.* **2009**, *5*, 618.
(22) Alicea, J. New directions in the pursuit of Majorana fermions in solid state systems. *Rep. Prog. Phys.* **2012**, *75*, 076501.
(23) Noh, C.; Rodŕıguez-Lara, B. M.; Angelakis, D. G. Proposal for realization of the Majorana equation in a tabletop experiment. *Phys. Rev. A* **2013**, *87*, 040102.
(24) Purcell, E. M.; Pennypacker, C. R. Scattering and absorption of light by nonspherical dielectric grains. *Astrophys. J.* **1973**, *186*, 705.
(25) Draine, B. T.; Flatau, P. J. Discrete-dipole approximation for scattering calculations. *J. Opt. Soc. Am. A* **1994**, *11*, 1491.
(26) Sukhorukov, A. A.; Kivshar, Y. S. Multigap discrete vector solitons. *Phys. Rev. Lett.* **2003**, *91*, 113902.
(27) Zeuner, J. M.; Efremidis, N. K.; Keil, R.; Dreisow, F.; Christodoulides, D. N.; Tünnermann, A.; Nolte, S.; Szameit, A. Optical analogues for massless dirac particles and conical diffraction in one dimension. *Phys. Rev. Lett.* **2012**, *109*, 023602.
(28) Malkova, N.; Ning, C. Z. Interplay between Tamm-like and Shockley-like surface states in photonic crystals. *Phys. Rev. B* **2007**, *76*, 045305.
(29) Heeger, A. J.; Kivelson, S.; Schrieffer, J. R.; Su, W. P. Solitons in conducting polymers. *Rev. Mod. Phys.* **1988**, *60*, 781−850.
(30) Johnson, P. B.; Christy, R. W. Optical constants of the noble metals. *Phys. Rev. B* **1972**, *6*, 4370−4379.
(31) Fujimoto, M. *The Physics of Structural Phase Transitions*; Springer: New York, 2010.
(32) Dousse, A.; Suffczynski, J.; Beveratos, A.; Krebs, O.; Lemaitre, A.; Sagnes, I.; Bloch, J.; Voisin, P.; Senellart, P. Ultrabright source of entangled photon pairs. *Nature* **2010**, *466*, 217−220.
(33) Liew, T. C. H.; Savona, V. Multimode entanglement in coupled cavity arrays. *New J. Phys.* **2013**, *15*, 025015.